Hindawi
Mathematical Problems in Engineering
Volume 2020, Article ID 7269809, 10 pages
https://doi.org/10.1155/2020/7269809

Research Article

A Semianalytical Solution for In-Plane Vibration Analysis of Annular Panels with Arbitrary Distribution of Internal Point Constraints

Peng Lyu, Jingtao Du, and Zhigang Liu

College of Power and Energy Engineering, Harbin Engineering University, Harbin 150001, China

Correspondence should be addressed to Jingtao Du; dujingtao@hrbeu.edu.cn

Received 7 December 2019; Revised 3 February 2020; Accepted 12 February 2020; Published 12 March 2020

Academic Editor: Calogero Orlando

Copyright © 2020 Peng Lyu et al. This is an open access article distributed under the Creative Commons Attribution License, which permits unrestricted use, distribution, and reproduction in any medium, provided the original work is properly cited.

In this paper, a semianalytical solution for the in-plane vibration analysis of annular panel with arbitrary distribution of internal point constraints is established for the first time. In-plane dynamic behavior of such panel structure is described via energy principle. A modified version of Fourier series is constructed for the in-plane vibration displacement expansion supplemented with the boundary smoothed terms, and the arbitrarily concentrated constraint in each field point is described in conjunction with Dirac delta function. A standard matrix eigenvalue problem containing various in-plane modal information of such annular panel is derived and solved through Rayleigh–Ritz procedure. Several numerical examples are presented to demonstrate the correctness and effectiveness of the proposed model by comparing the results with those from other approaches. Three representative types of point constraints, including point, line, and area configurations, are considered by collection of point constraints, and it is shown that the current model can make an accurate and efficient modal parameter prediction for annular panel with such most general case of point constraints.

1. Introduction

It is well known that the thin-walled plate structure is extensively used in various engineering branches, such as aerospace, shipbuilding, and automotive engineering. In the meanwhile, annular panel is also often encountered in many occasions severing as one of the important structural or device elements. Therefore, investigation on its vibration characteristics is considered as an important work with the aim to achieve an optimal design of relevant complex systems. For a single panel, its vibrational motion can be divided into two categories, namely, transverse and in-plane vibrations, according to the displacement direction with respect to the midplane of plate structure. Due to the possible reason of relatively lower bending flexibility related to the flexural vibration, which means that the resonant frequency of such vibration component tends to coincide with the surrounding excitations, transverse vibration has attracted a huge amount of research attention [1–4], compared with the study of its in-plane counterpart.

In recent years, under different backgrounds, such as rectangular plates [5, 6], elliptical plates [7], circular arches [8], and functionally graded plates [9], the in-plane vibration mode is gradually considered. In particular, the coupling effect of in-plane vibration in composite plate cannot be ignored [10, 11]. However, the high-order plate theory, which has the advantage of accuracy in laminated thick plate structures, increases the calculation amount but fails to improve the calculation accuracy for thin plate structures (panels). Moreover, the influence of in-plane mode on vibration energy transmission [12] and its application in ultrasonic motor [13] have attracted attention. Then, there is an increasing trend that much more efforts are devoted to the in-plane vibration study of plate structure, some of which are about the annular circular panels. In the earlier study, Ambati et al. and Irie et al. [14, 15] analyzed the in-plane vibration frequency and mode of annular plate in free state by using the transfer matrix method, and the results were verified by experimental measurement. Subsequently, in-plane vibration analysis of annular panels under various classical boundary conditions, such as clamped, was further examined by Farag and Pan, Park, and Bashmal et al. who made a lot of academic contribution on this topic [16–18]. Kim et al. [19] further extended and solved such boundary-value problem and for the general elastic edge restraints. Meanwhile, in-plane vibration of annular plate with other complex boundary conditions was also explored, such as the study of single-point boundary constraints conducted by Bashmal et al. [20]. In addition to the homogeneous material cases, with the development of material science and engineering, in-plane vibration of annular plates made of various novel composite materials is also investigated to obtain a deep understanding on dynamic characteristics of this vibration form. For example, Hosseini-Hashemi et al. and Lyu et al. [9, 21] explored the in-plane vibration of annular panels made of the functional gradient materials. Moreover, circular/annular plates are frequently encountered in various rotating machinery, and many research efforts are also made for the in-plane vibration analysis of rotating annular plate, such as the works by Chen and Jhu, Hamidzadeh, and Lyu et al. [22–24].

From the above in-plane vibration studies of annular panels, it can be found that most of the current work is mainly limited to the classical boundary conditions or uniform elastic constraints. However, in some practical engineering, the constraining conditions of plate structure may be not just confined to these traditional cases [25]. The traditional classic boundary constraints cannot completely accurately describe all the situations, such as bolts or rivets commonly encountered in the connection of plate structures. The connection through point coupling is often found in the interior of plate, instead of the boundary edge. So, it is necessary to establish the analysis model of plate structures with internal constraints. For example, there exist many studies on the transverse vibration analysis of plate structures with internal load and constraints. Starovoitov and Leonenko [26] examined the axisymmetric transverse vibration of a circular flexible sandwich plate with surface loads. Zhao et al. [27] carried out the vibration analysis of plates with complex and irregular support conditions by using the discrete singular convolution (DSC) method. Then, Civalek and Acar applied this method for the bending analysis of Mindlin plates on two-parameter elastic foundations [28]. However, this method only involves simple or clamped boundary, and some difficulties still exist in dealing with the case of free boundary. Liew and Wang [29] presented an investigation into the vibration characteristics of in-plane loaded rectangular plates with internal supports of arbitrary contour. All these studies show that the internal constraints can also have a significant influence on its dynamic behavior of plate structure. However, literature survey shows that there is little research effort devoted to in-plane vibration problem of annular panel taking the internal constraints into account. Moreover, when the fastening bolts or rivets become loose, the constraint is not clamped or completely free. Therefore, the intermediate state between clamped and free cases, namely, the elastic constraint, should be taken into account. For this

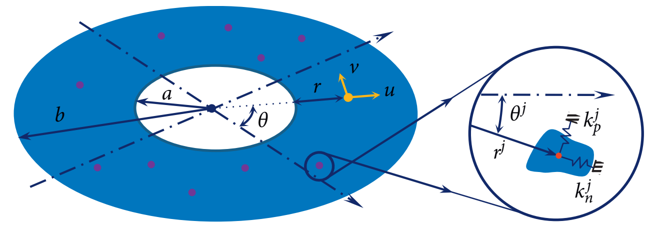

Figure 1: In-plane vibration of an annular panel with arbitrary distribution of internal point constraints.

problem, although the finite element method may be used to perform the vibration characteristics analysis of annular panel with such complex constraint conditions, any change of geometrical parameter or boundary restraint will need rebuilding of the FEM model, and with the increase of analysis frequency, a refined meshing is usually required. For this reason, there is an obvious need to develop an analytical-type model for the in-plane vibration analysis of annular panels with arbitrary internal constraints.

In this work, motivated by such limitation in literature, an attempt is made to tackle the in-plane vibration analysis of annular panel with internal constraint via a modified Fourier series expansion. The concentrated constraint in each field point is described through the Dirac delta function, and it is introduced into the system energy formulation in terms of potential energy. In conjunction with the Rayleigh–Ritz procedure, a system characteristic matrix is obtained and solved, from which the in-plane modal parameters are easily obtained. Several numerical examples are then presented to illustrate the correctness and reliability of the proposed model by comparing the results with those calculated from finite element analysis (FEA). Since all these internal constraints are described in a unified pattern in current framework, the internal point constraint can be extended to arbitrary shape on annular panel surface. The effectiveness of this model for the treatment of line constraint and local area constraint is verified repeatedly, and some data are obtained for the first time, which can be used as the validation benchmark for other future model development of in-plane vibration analysis of an annular panel with complex constraining conditions.

2. Mathematical Formulations

As shown in Figure 1, consider the in-plane vibration of an annular plate structure; in this work, the polar coordinate system is employed for the plate vibration modeling, which is also illustrated in this figure. In-plane vibration displacement of this annular plate can be represented as $u\,(r, \theta)$ and $v\,(r, \theta)$. It should be noted that r is the distance from the point in the annular panel to the inner edge, not the polar radius value. The value of r is the polar radius minus the inner radius a, and its value range is $r \in [0, \mathrm{R}]$, in which R is the radial span of the annular panel model namely, $R = \mathrm{B} - \mathrm{a}$. The red dots in this figure indicate the point constraints at any position across the annular panel. The elastic springs k_n^j and k_p^j are introduced to simulate the orthogonal radial and circumferential constraints, and the Dirac delta functions $k_n{}^j\delta\,(r-r^j,\ \theta-\theta^j)$ and $k_p{}^j\delta\,(r-r^j,\ \theta-\theta^j)$ are employed to describe the spatial distribution of point constraints inside the annular panel.

For structural vibration problem, dynamic description based on energy principle is one of the most commonly used methods. And it has significant advantages, when the structure or constraints are more complicated. For the in-plane vibration system of annular panel with arbitrary distribution of internal point constraints, the system Lagrangian function is

$$L = V - T, \tag{1}$$

where V and T are the total potential energy and kinetic energy of the in-plane vibration of annular panel structure, respectively. The total potential energy comprises two parts, namely: $V = V_p + V_s$, where V_s is the strain energy caused by the in-plane deformation of annular panel and V_p is the elastic potential energy stored by elastically constrained springs.

In the polar coordinate system, the in-plane strain energy of annular panel can be expressed as [18]

$$V_s = \frac{1}{2}h\int_0^R\int_0^{2\pi}\left(\sigma_r\varepsilon_r + \sigma_\theta\varepsilon_\theta + 2\sigma_{r\theta}\varepsilon_{r\theta}\right)(r+a)\mathrm{d}\theta\mathrm{d}r, \tag{2}$$

where h is the annular panel thickness; ε_r, ε_θ, and $\varepsilon_{r\theta}$ are the radial, circumferential, and shear stresses, respectively; and σ_r, σ_θ, and $\sigma_{r\theta}$ are the corresponding strains.

According to the plane elasticity theory, the relationship between the in-plane strain-stress and displacement of annular circular panel can be written down [18]:

$$\varepsilon_r = \frac{\partial u}{\partial r}, \tag{3}$$

$$\varepsilon_\theta = \frac{1}{r+a}\left(u + \frac{\partial v}{\partial \theta}\right), \tag{4}$$

$$\varepsilon_{r\theta} = \frac{1}{2}\left(\frac{1}{r+a}\frac{\partial u}{\partial \theta} + \frac{\partial v}{\partial r} - \frac{v}{r+a}\right), \tag{5}$$

$$\sigma_r = \frac{E}{1-\mu^2}\left(\frac{\partial u}{\partial r} + \frac{\mu u}{r+a} + \frac{\mu}{r+a}\frac{\partial v}{\partial \theta}\right), \tag{6}$$

$$\sigma_\theta = \frac{E}{1-\mu^2}\left(\mu\frac{\partial u}{\partial r} + \frac{u}{r+a} + \frac{1}{r+a}\frac{\partial v}{\partial \theta}\right), \tag{7}$$

$$\sigma_{r\theta} = \frac{E}{2(1+\mu)}\left(\frac{1}{r+a}\frac{\partial u}{\partial \theta} + \frac{\partial v}{\partial r} - \frac{v}{r+a}\right). \tag{8}$$

Substituting equations (3)–(8) into equation (2), one will obtain the in-plane strain energy V_s of annular panel in terms of its displacement fields, namely,

$$\begin{aligned} V_s = \frac{1}{2}h\int_0^R\int_0^{2\pi}\frac{E}{1-\mu^2}\Bigg[&\left(\frac{\partial u}{\partial r}\right)^2 + \frac{2\mu u}{r+a}\frac{\partial u}{\partial r} + \frac{2\mu}{r+a}\frac{\partial v}{\partial \theta}\frac{\partial u}{\partial r} + \frac{u^2}{(r+a)^2} + \frac{2u}{(r+a)^2}\frac{\partial v}{\partial \theta} + \frac{1}{(r+a)^2}\left(\frac{\partial v}{\partial \theta}\right)^2 + \frac{1-\mu}{2}\left(\frac{1}{r+a}\frac{\partial u}{\partial \theta}\right)^2 \\ &+ \frac{1-\mu}{2}\left(\frac{\partial v}{\partial r}\right)^2 + \frac{1-\mu}{2}\left(\frac{v}{r+a}\right)^2 + \frac{1-\mu}{r+a}\frac{\partial u}{\partial \theta}\frac{\partial v}{\partial r} - \frac{1-\mu}{(r+a)^2}\frac{\partial u}{\partial \theta}v - \frac{1-\mu}{r+a}\frac{\partial v}{\partial r}v\Bigg](r+a)\mathrm{d}\theta\mathrm{d}r, \end{aligned} \tag{9}$$

where E and μ are Young's modulus and Poisson's ratio of this elastic annular panel, respectively.

The elastic potential energy V_p stored in various elastic point restraining springs can be expressed as

$$V_p = \frac{1}{2}\int_0^{2\pi}\int_0^R\left(\begin{array}{c}\sum\limits_{j=1}^{J}k_n^j\delta\left(r-r^j,\theta-\theta^j\right)u^2 \\ +\sum\limits_{j=1}^{J}k_p^j\delta\left(r-r^j,\theta-\theta^j\right)v^2\end{array}\right)(r+a)\mathrm{d}\theta\mathrm{d}r, \tag{10}$$

where J is the total number of elastic point constraints. It should be pointed out that since the arbitrary distribution of elastic point constraints is accounted for in such a general pattern, any shape and position for the constraint configuration can be readily treated in such summation way of elastic potential energies associated with each point constraints of any restraining stiffness.

In-plane kinetic energy T of annular panel will be

$$T = \frac{1}{2}\rho h\omega^2\int_0^R\int_0^{2\pi}\left(u^2+v^2\right)(r+a)\mathrm{d}\theta\mathrm{d}r, \tag{11}$$

where ρ is the mass density of panel material and ω is the circular frequency.

For the energy formulation of in-plane vibration of annular panel, with the aim to derive the accurate enough system characteristic parameters, it is necessary to construct the sufficiently smooth vibration displacement field functions. For the vibration analysis of annular panel with inner and outer edges, the standard Fourier series is usually used for the expansion of radial component of the displacement function under classical boundary condition. For the general elastic constraints considered in this work, the traditional Fourier series expression will not satisfy the differential smoothness requirement. In order to overcome the spatial derivative discontinuity associated with the standard Fourier series radial component at general boundaries, supplementary polynomial functions will be superimposed to the original series assumption. Thus, the boundary smoothed in-plane vibration displacement field functions of the annular panel are given as follows:

$$u(r,\theta) = \left[\sum_{m=0}^{\infty}\sum_{n=0}^{\infty} A_{\mathrm{mn}}\cos(\lambda_{\mathrm{am}}r)\cos(n\theta) + \sum_{m=0}^{\infty}\sum_{n=1}^{\infty} B_{\mathrm{mn}}\cos(\lambda_{\mathrm{am}}r)\sin(n\theta) + \sum_{n=0}^{\infty} a_n\xi_{1r}(r)\cos(n\theta) + \sum_{n=1}^{\infty} b_n\xi_{1r}(r)\sin(n\theta) + \sum_{n=0}^{\infty} c_n\xi_{2r}(r)\cos(n\theta) + \sum_{n=1}^{\infty} d_n\xi_{2r}(r)\sin(n\theta)\right]e^{i\omega t}, \tag{12a}$$

$$v(r,\theta) = \left[\sum_{m=0}^{\infty}\sum_{n=0}^{\infty} C_{\mathrm{mn}}\cos(\lambda_{\mathrm{am}}r)\cos(n\theta) + \sum_{m=0}^{\infty}\sum_{n=1}^{\infty} D_{\mathrm{mn}}\cos(\lambda_{\mathrm{am}}r)\sin(n\theta) + \sum_{n=0}^{\infty} e_n\xi_{1r}(r)\cos(n\theta) + \sum_{n=1}^{\infty} f_n\xi_{1r}(r)\sin(n\theta) + \sum_{n=0}^{\infty} g_n\xi_{2r}(r)\cos(n\theta) + \sum_{n=1}^{\infty} h_n\xi_{2r}(r)\sin(n\theta)\right]e^{i\omega t}, \tag{12b}$$

where $\lambda_{\mathrm{am}} = m\pi/R$ and

$$\xi_{1r}(r) = R\frac{r}{R}\left(\frac{r}{R}-1\right)^2, \qquad \xi_{2r}(r) = R\left(\frac{r}{R}\right)^2\left(\frac{r}{R}-1\right). \tag{13}$$

In this way, the first-order derivative of the displacement function at the boundary will no longer be equal to zero and thus possess the ability to express internal forces in case of arbitrary elastic constraints; then, the accuracy and convergence of the constructed series solution are improved. In fact, the construction of supplementary function is not unique, and the main purpose of such supplementary terms is just to make the relevant derivative associated with displacement function sufficiently continuous in the whole solving domain including the general boundaries.

Substituting the modified Fourier series expansion of in-plane displacement function equations (12a) and (12b) into the system energy formulation equations (9)–(11), truncating all the series expansions to M and N, respectively, and minimizing the system Lagrangian L with respect to all the unknown coefficient, namely, $\partial L/\partial X = 0$, one will obtain the system characteristic equation in the matrix form, namely,

$$\left(\mathbf{K} - \omega^2\mathbf{M}\right)\mathbf{X} = 0, \tag{14}$$

where $\mathbf{K}$ and $\mathbf{M}$ are the stiffness and mass matrices of $(2M+6)\times(2\mathrm{N}+1)$, and

$$\mathbf{X} = \left[\mathbf{X}_A, \mathbf{X}_B, \mathbf{X}_a, \mathbf{X}_b, \mathbf{X}_c, \mathbf{X}_d, \mathbf{X}_C, \mathbf{X}_D, \mathbf{X}_e, \mathbf{X}_f, \mathbf{X}_g, \mathbf{X}_h\right]^{\mathrm{T}}, \tag{15}$$

$$\mathbf{X}_A = [A_{00}, \ldots A_{M0}, \ldots\ldots, A_{\mathrm{MN}}], \tag{16a}$$

$$\mathbf{X}_B = [B_{01}, \ldots B_{M1}, \ldots\ldots, B_{\mathrm{MN}}], \tag{16b}$$

$$\mathbf{X}_a = [a_0, \ldots a_N], \tag{17a}$$

$$\mathbf{X}_b = [b_1, \ldots b_N], \tag{17b}$$

$$\mathbf{X}_c = [c_0, \ldots c_N], \tag{17c}$$

$$\mathbf{X}_d = [d_1, \ldots d_N], \tag{17d}$$

$$\mathbf{X}_C = [C_{00}, \ldots C_{M0}, \ldots\ldots, C_{\mathrm{MN}}], \tag{18a}$$

$$\mathbf{X}_B = [D_{01}, \ldots D_{M1}, \ldots\ldots, D_{\mathrm{MN}}], \tag{18b}$$

$$\mathbf{X}_e = [e_0, \ldots e_N], \tag{19a}$$

$$\mathbf{X}_f = [f_1, \ldots f_N], \tag{19b}$$

$$\mathbf{X}_g = [g_0, \cdots g_N], \tag{19c}$$

$$\mathbf{X}_h = [h_1, \ldots h_N]. \tag{19d}$$

Table 1: The first eight in-plane modal frequencies of annular panel with a single-point fixed constraint.

Methods	Modal frequencies (Hz)							
	f_1	f_2	f_3	f_4	f_5	f_6	f_7	f_8
FEA	0.0001	573.73	952.49	1523.6	1604	2584.5	2827.8	2873.5
$k = 0$	0.0005	0.0014	0.2970	1249.0	1249.0	2514.2	2802.3	2802.3
$k = 1e5$	0.2042	0.4151	0.6036	1249.0	1249.0	2514.2	2802.3	2802.3
$k = 1e8$	0.2186	13.123	17.827	1249.0	1249.1	2514.2	2802.3	2802.4
$k = 1e10$	0.2186	128.94	176.65	1252.1	1260.0	2517.5	2803.2	2807.6
$k = 1e11$	0.2186	353.65	515.58	1281.4	1345.0	2540.2	2809.9	2842.3
$k = 1e12$	0.2186	579.11	946.21	1513.6	1613.4	2585.8	2827.4	2873.9
	—	0.94%	0.66%	0.66%	0.58%	0.05%	0.01%	0.01%

By solving such a standard matrix eigenvalue problem equation (14), one can obtain all the in-plane modal characteristics of annular plate with an arbitrary number of elastic point constraints. The corresponding physical mode shapes can be easily calculated by substituting the corresponding eigenvector into the modified Fourier series expansion of in-plane vibration displacement of annular panel equations (12a) and (12b).

3. Numerical Results and Discussion

In this section, several numerical examples will be presented to verify the correctness and effectiveness of the established model in comparison with those calculated from finite element analysis. Here, material and geometrical parameters are selected as follows: Young's modulus $E = 2.1 \times 10^{11}$ Pa, Poisson's ratio $\mu = 0.3$, mass density $\rho = 7800\ \mathrm{kg/m^3}$, and inner and outer radii a and b are 0.2 m and 0.5 m, respectively. Since the improved Fourier series expressions equations (12a) and (12b) are sufficiently smooth in the whole solving domain, the rapid convergence characteristics has been obtained. Various truncated terms have been used for the convergence study, and it was found that the use of $M = 15$ can guarantee the solution convergence and accuracy. In all the subsequent calculations, such truncated number will be used.

3.1. Point Constraint. As the first example, let us consider the in-plane vibration of annular panel with a single-point fixed constraint. The constraint point position is (0.35, 0) in the polar coordinate. In current modeling framework, the point fixed constraint can be realized by setting the restraining stiffnesses into both extremely large numbers along the radial and circumferential directions. Tabulated in Table 1 are the first eight in-plane modal frequencies of this annular panel, in which the modal frequencies computed under various spring stiffnesses are given. With the aim of comparison, FEA results are also presented for such point fixed constraint. It can be observed that with the increase of restraining stiffness, the frequency parameters from these two methods can coincide well with each other. Then, the restraining stiffness $k_n = k_p = 1E12$ is large enough to represent such rigid point constraint, and the correctness of current model for prediction of in-plane modal characteristics of annular panel with such single-point fixed constraint is then validated. By substituting the corresponding

Table 2: Comparison of the first eight mode shape of annular plate with a single-point fixed constraint by using these two methods.

	FEA	Present
1st		
2nd	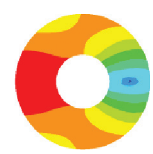	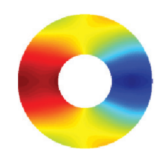
3rd	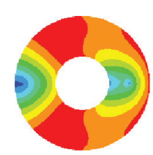	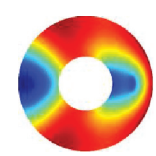
4th	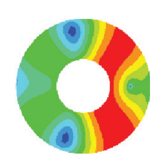	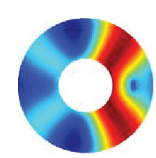
5th	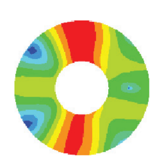	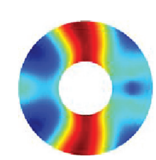
6th	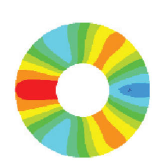	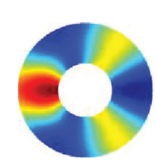

Table 2: Continued.

	FEA	Present
7^{th}	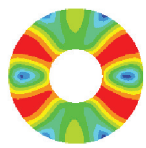	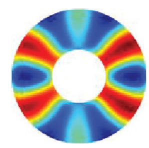
8^{th}	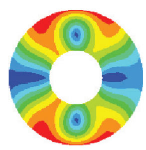	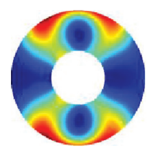

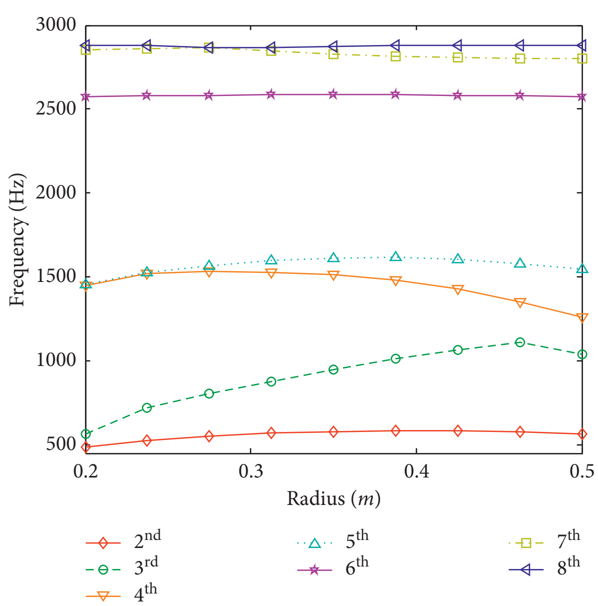

Figure 2: Variation of the first eight in-plane modal frequencies of annular panel with respect to the point constraint position along the radial direction.

eigenvector into the constructed displacement function equations (12a) and (12b), one can get the physical mode shapes. Tabulated in Table 2 is the comparison of the first eight in-plane mode shapes; again, one can find that the agreement between these two results is satisfactory.

In order to further examine the influence of point constraint on the in-plane modal frequency of this annular panel, variation of the first eight natural frequencies with the applied position of point constraint along the radial direction is shown in Figure 2. Here, the first in-plane frequency parameter is not given, which corresponds to the rigid body motion of annular panel swinging around such point constraint. From this figure, it can be seen that the position of point constraint has a significant effect on some relative

Table 3: The first eight in-plane modal frequencies of annular panel with four-point constraints.

Modal frequencies	FEA	Present	Difference
f_1	1623.7	1623.4	0.02
f_2	1682.5	1688.4	0.35
f_3	1720.1	1760.0	2.32
f_4	1738.4	1760.0	1.24
f_5	2591.8	2671.4	3.07
f_6	2892.2	2894.7	0.09
f_7	2892.8	2894.7	0.07
f_8	2932.9	2947.0	0.48

lower-order modal frequencies, such as the third-order mode. Then, it is of great importance to determine the point constraint position in the engineering practice for structural vibration frequency assignment of such plate structure.

For this modeling approach, multiple point constraints can be considered straightforwardly by including the corresponding elastic energies in the system Lagrangian. Four-point constraints as (0.35, 0), (0.35, $\pi/2$), (0.35, π), and (0.35, $3\pi/2$) in the polar coordinate will be considered first. Since there are no data available in current literature, finite element analysis is employed to make a prediction for the comparison purpose, and the first eight in-plane modal frequencies are presented in Table 3. We can see that these results are in good agreement with those calculated from finite element analysis. Then, the correctness and effectiveness of the proposed model for predicting the in-plane modal characteristics of annular panel with multiple point constraints are validated.

3.2. Line Constraint

3.2. Line Constraint. One of the constraint forms usually encountered in various engineering occasions is the line constraint, which can be viewed as a collection of point constraints. In this section, two types of line constraints will be taken into account; for comparison, the results calculated by using finite element analysis are also presented to verify the accuracy of the proposed model.

3.2.1. Case I. In Case I, the constrained position is described as $r \in [a, b]$, $\theta = 0$ in the polar coordinate system, and comparison of in-plane modal frequencies and the corresponding mode shapes is presented in Tables 4 and 5, respectively. As the number of constraint points increases, the modal frequency parameter gradually approaches to the finite element calculation result. These two results obtained by both two methods are almost the same, when the number of constraint points is close to the number of nodes for the line in finite element analysis.

3.2.2. Case II. Now, another more arbitrary form of line constraint Case II is analyzed, the polar coordinates of which are expressed as $r = 2R\theta/\pi$, $\theta \in [0, \pi/2]$. The in-plane modal frequency and mode shape results are presented in Tables 6 and 7. It can be seen again that the comparison with these results obtained by the both two methods can agree very well with each other, and then the correctness of the current

Table 4: In-plane modal frequency of annular panel with the line constraint of Case I.

	f_1	f_2	f_3	f_4	f_5	f_6	f_7	f_8
FEA	280.72	660.09	1205.7	1797.7	2293.2	2608.5	2885.2	3095.2
11p	266.19	661.5	1200.7	1798.4	2227.4	2608.5	2886.3	3052.7
	5.18%	0.21%	0.41%	0.04%	2.87%	0.00%	0.04%	1.37%
15p	271.64	663.07	1204.8	1803.3	2251.9	2609	2886.5	3066.9
	3.23%	0.45%	0.08%	0.31%	1.80%	0.02%	0.05%	0.91%
19p	274.81	663.98	1207.2	1806.1	2265.4	2609.2	2886.7	3075.5
	2.11%	0.59%	0.13%	0.47%	1.21%	0.03%	0.05%	0.63%
23p	276.92	664.57	1208.9	1808	2274.1	2609.4	2886.8	3081.4
	1.35%	0.68%	0.27%	0.57%	0.83%	0.03%	0.06%	0.45%
27p	278.44	664.99	1210.2	1809.3	2280.2	2609.5	2886.9	3085.7
	0.81%	0.74%	0.37%	0.64%	0.57%	0.04%	0.06%	0.31%
31p	279.6	665.3	1211.1	1810.2	2284.7	2609.6	2887	3089
	0.40%	0.79%	0.45%	0.70%	0.37%	0.04%	0.06%	0.20%
35p	280.52	665.55	1211.9	1811	2288.2	2609.7	2887	3091.7
	0.07%	0.83%	0.52%	0.74%	0.22%	0.05%	0.06%	0.11%

Table 5: In-plane mode shapes of annular panel with the line constraint of Case I.

	FEA	Present
1st		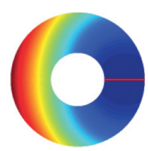
2nd		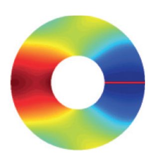
3rd		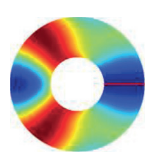
4th	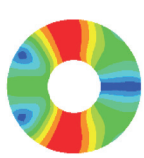	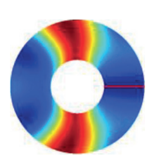
5th	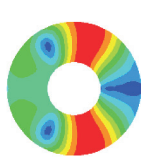	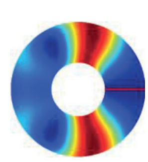

Table 5: Continued.

	FEA	Present
6th		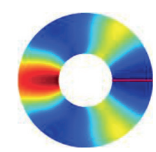
7th	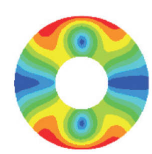	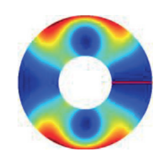
8th	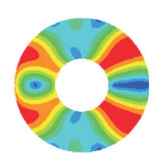	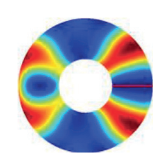

method for the analysis of in-plane modal characteristics of annular panel with such general line constraint case can be verified.

It should be noted that the familiar boundary restraint can be seen as a special type of line constraint, which has been one of the research focuses for many years. In the current analysis method, when the constraint coordinates are set to locate on its edges, the in-plane vibration characteristic investigation under various boundary conditions can be easily performed like the aforementioned line constraint.

Table 6: In-plane modal frequency of annular panel with the line constraint of Case II.

	f_1	f_2	F_3	f_4	f_5	f_6	f_7	f_8
FEA	435.72	966.47	1605.6	2084.4	2561.3	2843.2	3264	3589.4
11p	422.93	946.41	1564.6	2045.2	2478.2	2830.7	3207.2	3540.2
	−1.95%	−1.53%	−1.93%	−1.38%	−2.33%	−0.33%	−1.16%	−1.08%
15p	426.51	952.77	1578.8	2058.9	2506.7	2834.8	3223.9	3558.9
	−1.12%	−0.87%	−1.03%	−0.72%	−1.21%	−0.18%	−0.64%	−0.56%
19p	428.66	956.53	1586.5	2066.1	2521.1	2837.2	3233.3	3568.3
	−1.62%	−1.03%	−1.19%	−0.88%	−1.57%	−0.21%	−0.94%	−0.59%
23p	430.17	959.15	1591.6	2070.7	2530.5	2838.8	3239.8	3574.5
	−1.27%	−0.76%	−0.87%	−0.66%	−1.20%	−0.15%	−0.74%	−0.42%
27p	431.33	961.12	1595.3	2073.9	2537.3	2840	3244.7	3578.9
	−1.01%	−0.55%	−0.64%	−0.50%	−0.94%	−0.11%	−0.59%	−0.29%
31p	432.27	962.69	1598.2	2076.3	2542.5	2840.9	3248.5	3582.2
	−0.79%	−0.39%	−0.46%	−0.39%	−0.73%	−0.08%	−0.47%	−0.20%
35p	433.05	963.98	1600.4	2078.2	2546.6	2841.7	3251.7	3584.8
	−0.61%	−0.26%	−0.32%	−0.30%	−0.57%	−0.05%	−0.38%	−0.13%

Table 7: In-plane mode shapes of annular panel with the line constraint of Case II.

	FEA	Present
1st		
2nd		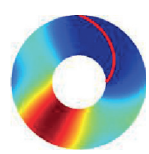
3rd	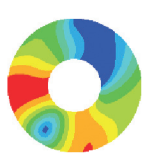	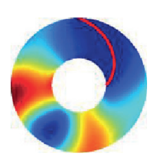
4th		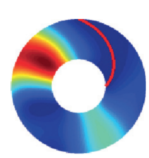
5th	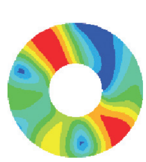	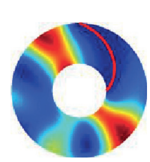

Table 7: Continued.

	FEA	Present
6th	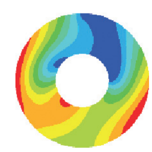	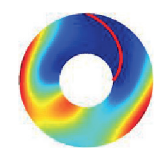
7th	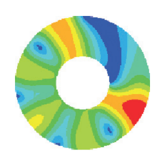	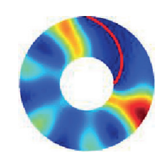
8th	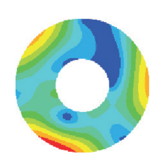	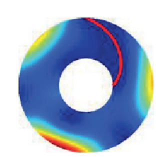

Table 8: In-plane modal frequencies of annular panel with a sector area constraint.

Modal frequencies	FEA	Present 36 points	Difference (%)
f_1	268.32	264.85	1.29
f_2	739.21	737.34	0.25
f_3	1329.6	1324.9	0.36
f_4	1952.8	1942.4	0.53
f_5	2313.0	2290.2	0.99
f_6	2662.1	2660.3	0.07
f_7	2992.7	2981.8	0.36
f_8	3222.3	3217.2	0.16

Table 9: The first eight mode shapes of annular panel with a sector area constraint.

	FEA	Present
1^{st}		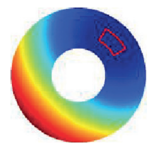
2^{nd}		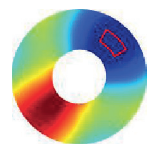
3^{rd}	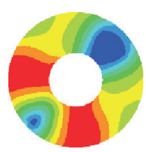	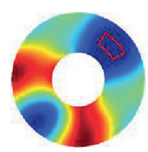
4^{th}		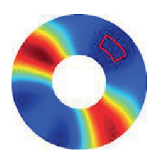
5^{th}	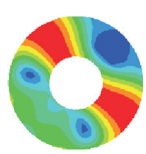	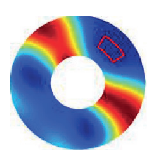
6^{th}	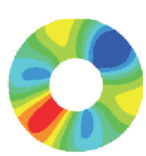	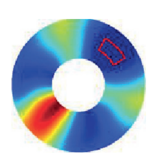
7^{th}	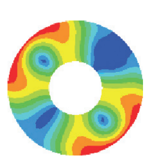	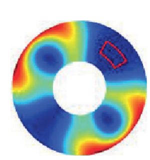
8^{th}	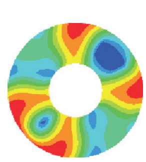	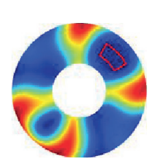

3.3. Local Area Constraint. In some practical engineering scenario, local constraints are inevitable. Therefore, as the last example, let us shift our attention to the in-plane vibration of annular panel under local area constraints. For such complex constraint type, there is little work done in the open literature. Here, finite element analysis will be employed for the modal parameter calculation, in which the local area constraint can be achieved by constraining all the nodes in the region. Then, an analysis example of the local area constraint of a sector is given, and its polar coordinate range is $r \in [0.3, 0.4]$, $\theta \in [\pi/6, \pi/3]$. 36 points are taken into account to represent this area. The comparisons of the frequency and mode shape are shown in Tables 8 and 9, respectively. From the tables, we can observe that the results are in good agreement. Although FEA can be used for such in-plane vibration analysis, the tedious task of re-modelling is always needed for any change of constraint condition, either the geometrical configuration or spatial distribution pattern, which makes that such method is not suitable for the parametric studies.

From the aforementioned various examples, it can be clearly found that the proposed method in this work is sufficiently accurate as well as effective to account for various complicated constraints, and the constraint of arbitrary position across the annular panel surface can be readily implemented.

4. Conclusions

In this paper, an accurate and efficient solution for the in-plane vibration analysis of annular panel with arbitrary distribution of internal point constraints is proposed and established for the first time. Energy principle is employed for the in-plane vibration description of the annular panel system. Several numerical examples are presented to illustrate the accuracy and effectiveness of the developed solution by comparing the results with those calculated from FEA. And the following conclusions are obtained:

(1) Arbitrary distribution of point constraints is accounted for through the introduction of its potential energy in conjunction with Dirac delta function. A modified version of Fourier series is constructed to express the in-plane vibration displacement, in which the auxiliary terms are supplemented to the displacement radial component to eliminate the derivative discontinuity on the inner and outer edges of annular panel.

(2) Unlike FEA, there is no need to change the simulation code too much, when any change of internal/boundary point constraints is of desire, since all the point constraints are treated in a unified pattern by including its relevant potential energy in system Lagrangian.

(3) Three types of point constraints are considered, namely, point, line, and area constraints, which can be obtained by a set of point constraints. Both the in-plane modal frequencies and mode shapes are predicted.

(4) This work for the first time proposes a semianalytical solution for the in-plane vibration analysis of

annular panel with an arbitrary distribution of internal point constraints, and some modal data are obtained for the first time, which can be used as the benchmark for other method development in future.

Data Availability

The data are available on request.

Conflicts of Interest

The authors declare that they have no conflicts of interest.

Acknowledgments

This study was supported by the National Natural Science Foundation of China (grant no. 11972125) and Fok Ying Tung Education Foundation (grant no. 161049).

References

[1] A. W. Leissa, *Vibration of Plates*, Acoustical Society of America, New York, NY, USA, 1993.

[2] T. Irie, G. Yamada, and K. Takagi, "Natural frequencies of thick annular plates," *Journal of Applied Mechanics*, vol. 49, no. 3, pp. 633–638, 1982.

[3] W. L. Li, "Vibration analysis of rectangular plates with general elastic boundary supports," *Journal of Sound and Vibration*, vol. 273, no. 3, pp. 619–635, 2004.

[4] J.-H. Kang, "Three-dimensional vibration analysis of thick, circular and annular plates with nonlinear thickness variation," *Computers & Structures*, vol. 81, no. 16, pp. 1663–1675, 2003.

[5] J. T. Du, W. L. Li, G. Y. Jin, T. J. Yang, and Z. G. Liu, "An analytical method for the in-plane vibration analysis of rectangular plates with elastically restrained edges," *Journal of Sound and Vibration*, vol. 306, no. 3-5, pp. 908–927, 2007.

[6] G. Wang and N. M. Wereley, "Free in-plane vibration of rectangular plates," *AIAA Journal*, vol. 40, no. 5, pp. 953–959, 2002.

[7] S. H. Hasheminejad, A. Ghaheri, and S. Vaezian, "Exact solution for free in-plane vibration analysis of an eccentric elliptical plate," *Acta Mechanica*, vol. 224, no. 8, pp. 1609–1624, 2013.

[8] P. Malekzadeh, M. M. Atashi, and G. Karami, "In-plane free vibration of functionally graded circular arches with temperature-dependent properties under thermal environment," *Journal of Sound and Vibration*, vol. 326, no. 3-5, pp. 837–851, 2009.

[9] S. Hosseini-Hashemi, M. Fadaee, and M. Es'haghi, "A novel approach for in-plane/out-of-plane frequency analysis of functionally graded circular/annular plates," *International Journal of Mechanical Sciences*, vol. 52, no. 8, pp. 1025–1035, 2010.

[10] S. Hosseini Hashemi, S. R. Atashipour, and M. Fadaee, "An exact analytical approach for in-plane and out-of-plane free vibration analysis of thick laminated transversely isotropic plates," *Archive of Applied Mechanics*, vol. 82, no. 5, pp. 677–698, 2012.

[11] A. Alaimo, C. Orlando, and S. Valvano, "Analytical frequency response solution for composite plates embedding viscoelastic layers," *Aerospace Science and Technology*, vol. 92, pp. 429–445, 2019.

[12] R. H. Lyon, "In-plane contribution to structural noise transmission," *Noise Control Engineering Journal*, vol. 26, no. 1, pp. 22–27, 1986.

[13] V. Dabbagh, A. A. D. Sarhan, J. Akbari, and N. A. Mardi, "Design and manufacturing of ultrasonic motor with in-plane and out-of-plane bending vibration modes of rectangular plate with large contact area," *Measurement*, vol. 109, pp. 425–431, 2017.

[14] G. Ambati, J. F. W. Bell, and J. C. K. Sharp, "In-plane vibrations of annular rings," *Journal of Sound and Vibration*, vol. 47, no. 3, pp. 415–432, 1976.

[15] T. Irie, G. Yamada, and Y. Muramoto, "Natural frequencies of in-plane vibration of annular plates," *Journal of Sound and Vibration*, vol. 97, no. 1, pp. 171–175, 1984.

[16] N. H. Farag and J. Pan, "Modal characteristics of in-plane vibration of circular plates clamped at the outer edge," *The Journal of the Acoustical Society of America*, vol. 113, no. 4, pp. 1935–1946, 2003.

[17] C. I. Park, "Frequency equation for the in-plane vibration of a clamped circular plate," *Journal of Sound and Vibration*, vol. 313, no. 1-2, pp. 325–333, 2008.

[18] S. Bashmal, R. Bhat, and S. Rakheja, "In-plane free vibration of circular annular disks," *Journal of Sound and Vibration*, vol. 322, no. 1-2, pp. 216–226, 2009.

[19] C.-B. Kim, H. S. Cho, and H. G. Beom, "Exact solutions of in-plane natural vibration of a circular plate with outer edge restrained elastically," *Journal of Sound and Vibration*, vol. 331, no. 9, pp. 2173–2189, 2012.

[20] S. Bashmal, R. Bhat, and S. Rakheja, "In-plane free vibration analysis of an annular disk with point elastic support," *Shock and Vibration*, vol. 18, no. 4, pp. 627–640, 2011.

[21] P. Lyu, J. Du, Z. Liu, and P. Zhang, "Free in-plane vibration analysis of elastically restrained annular panels made of functionally graded material," *Composite Structures*, vol. 178, no. 15, pp. 246–259, 2017.

[22] J. S. Chen and J. L. Jhu, "On the in-plane vibration and stability of a spinning annular disk," *Journal of Sound and Vibration*, vol. 195, no. 4, pp. 585–593, 1996.

[23] H. R. Hamidzadeh, "In-plane free vibration and stability of rotating annular discs," *Proceedings of the Institution of Mechanical Engineers, Part K: Journal of Multi-Body Dynamics*, vol. 216, no. 4, pp. 371–380, 2002.

[24] P. Lyu, J. Du, Y. Wang, and Z. Liu, "Free in-plane vibration analysis of rotating annular panels with elastic boundary restraints," *Journal of Sound and Vibration*, vol. 439, pp. 434–456, 2019.

[25] W. H. Yang, "Vibration of a plate with internal constraints," *Journal of Applied Mechanics*, vol. 41, no. 4, pp. 1072–1074, 1974.

[26] E. I. Starovoitov and D. V. Leonenko, "Vibrations of circular composite plates on an elastic foundation under the action of local loads," *Mechanics of Composite Materials*, vol. 52, no. 5, pp. 665–672, 2016.

[27] Y. B. Zhao, G. W. Wei, and Y. Xiang, "Plate vibration under irregular internal supports," *International Journal of Solids and Structures*, vol. 39, no. 5, pp. 1361–1383, 2002.

[28] Ö. Civalek and M. H. Acar, "Discrete singular convolution method for the analysis of Mindlin plates on elastic foundations," *International Journal of Pressure Vessels and Piping*, vol. 84, no. 9, pp. 527–535, 2007.

[29] K. M. Liew and C. M. Wang, "Flexural vibration of in-plane loaded plates with straight line/curved internal supports," *Journal of Vibration and Acoustics*, vol. 115, no. 4, pp. 441–447, 1993.